

Comparison of Cryogenic Radiometry and Thermal Radiometry Calibrations at NIST using Multichannel Filter Radiometers

B. Carol Johnson, Steven W. Brown, Keith R. Lykke, and Charles E. Gibson

*Optical Technology Division
National Institute of Standards and Technology
100 Bureau Drive, MS 8441
Gaithersburg, MD 20899-8441 USA*

Giulietta Fargion and Gerhard Meister

*SIMBIOS Project, Code 970.2
NASA Goddard Space Flight Center
Greenbelt, Maryland 20771 USA*

Stanford B. Hooker

*Laboratory for Hydrospheric Processes, Code 970.2
NASA Goddard Space Flight Center
Greenbelt, Maryland 20771 USA*

Brian Markham

*Landsat Project Science Office, Code 923
NASA Goddard Space Flight Center
Greenbelt, Maryland 20771 USA*

James J. Butler

*EOS Project Science Office, Code 925
NASA Goddard Space Flight Center
Greenbelt, Maryland 20771 USA*

Principal Contact: B. Carol Johnson, Tel.: 1 301 975-2322, Fax.: 1 301 869 5700, e-mail: cjohnson@nist.gov

Abstract. Comparison of independent measurement results allow an assessment of the accuracy of the underlying methods. In this work, four multichannel filter radiometers were calibrated using tunable laser-illuminated and lamp-illuminated integrating sphere sources (ISSs). The determination of the radiance of the laser-illuminated ISS is based on electrical substitution radiometry at cryogenic temperatures and dimensional metrology of circular apertures. The determination of the spectral radiance of the lamp-

illuminated ISS is based on blackbody physics, referenced to the freezing temperature of gold. By calibrating the filter radiometers using both methods, we compare the “detector-based” to the “source-based” radiance scale at the National Institute of Standards and Technology (NIST).

Key Words: absolute radiometry; calibration; Earth Observing System; filter radiometers; integrating sphere sources; remote sensing; spectral radiance

1. Introduction

Realization of radiometric quantities using new methods based on electrical substitution radiometry and dimensional metrology has resulted in reduced uncertainties compared to methods based on temperature scales and blackbody physics. The methods are referred to as “detector-based” and “source-based” radiometry, respectively, reflecting the different transfer standards used. At NIST, the spectral radiance values assigned to lamp-illuminated integrating sphere sources (ISSs) are determined by reference to a gold-point blackbody. Such lamp-illuminated ISSs are often used to calibrate radiometers. A detector-based method of calibrating a radiometer that incorporates a laser-illuminated ISS is also possible at NIST, resulting in the absolute radiance (or irradiance) responsivity at an arbitrary number of discrete wavelengths within the instrument’s bandpass.

When a filter radiometer, calibrated using the detector-based method, is used to measure broadband sources such as lamp-illuminated integrating spheres, the radiance responsivity, multiplied by the source spectral radiance and integrated over wavelength,

predicts the signal that should be observed. We used four multichannel filter radiometers designed for radiance measurements and a large area lamp-illuminated source to compare the two techniques. Use of narrow field-of-view filter radiometers, calibrated using the more accurate laser technique, to determine the temperature of a small-aperture, high-emittance variable-temperature blackbody is a method to generate a detector-based spectral radiance scale. Hence this work also gave us experience in the steps required to implement a detector-based spectral radiance scale at NIST, similar to that accomplished recently in spectral irradiance [1].

2. Instrument and facility descriptions

Here we describe the relevant properties of the filter radiometers and the two methods used to calibrate them. The multichannel filter radiometers are used to validate the spectral radiance values assigned to large-area integrating sphere sources, such as those used to calibrate satellite sensors in the Earth Observing System (EOS) prior to launch [2]. The optical design of each radiometer is similar, with six independent channels, a commercial camera objective lens, and an electronic interface for data acquisition. The filters and detectors are temperature stabilized. At a 1 m working distance, the target diameter is about 50 mm.

The SeaWiFS Transfer Radiometer (SXR) [3] was built to support calibration efforts in an ocean color satellite program, the Sea-viewing Wide Field-of-view Sensor (SeaWiFS). The Visible Transfer Radiometer (VXR) [4] is used in EOS calibration intercomparisons. The LandSat Transfer Radiometer (LXR) [5] is part of the Enhanced Thematic Mapper Plus (ETM+) calibration program. The SXR-II is used for source

comparisons [6] in the Sensor Intercomparison and Merger for Biological and Interdisciplinary Ocean Studies (SIMBIOS) program.

The center wavelengths (between 412 nm and 870 nm) and bandwidths (about 10 nm) in the SXR, VXR, and SXR-II correspond to a subset of those used for ocean science products. Likewise in the LXR, four channels correspond to a subset of the ETM+ channels; they are broadband (60 nm to 100 nm) with center wavelengths of 481 nm, 560 nm, 661 nm, and 821 nm. The interference filters in the remaining two LXR channels have the same design specifications as the 441 nm and 662 nm filters in the other three radiometers. Aside from the difference in the bandwidths, the pre-amp gains in the SXR and SXR-II were chosen for lower level sources compared to the VXR and LXR. Consequently, the SXR and SXR-II saturate before the VXR and LXR.

The Spectral Irradiance and Radiance Responsivity Calibrations with Uniform Sources (SIRCUS) facility [7] was used to determine the absolute radiance responsivity at many wavelengths in both the in-band and out-of-band region of each channel for all four filter radiometers. In SIRCUS, the radiometers viewed a laser-illuminated ISS that provided a known source of monochromatic radiance. The laser-illuminated ISS method offers several advantages, including spectral purity, wavelength accuracy, and high radiance levels, compared to the lamp-illuminated ISS method, resulting in reduced uncertainties [4]. The radiance was determined using a trap detector that was calibrated using a cryogenic radiometer and measurements of the relevant aperture areas and distance. A wide variety of tunable lasers provided coverage from 380 nm to 920 nm.

The NIST Facility for Automated Spectral Radiance Calibrations (FASCAL) [8] was used to calibrate a lamp-illuminated ISS for spectral radiance from 300 nm to

1100 nm by comparison with a variable temperature blackbody. A prism-grating spectroradiometer with reflective foreoptics, a 0.6 mm by 0.8 mm target area, and a wavelength-dependent dispersion (maximum value of 3.7 nm/mm at 800 nm) is used to transfer the spectral radiance of a variable temperature blackbody to the ISS. The temperature of the blackbody is determined by reference to a ribbon filament lamp, which is referenced to a gold-point blackbody. The lamp-illuminated ISS we calibrated was the EOS/NIST Portable Radiance Source (NPR) [9], a 30 cm diameter, internally illuminated, Spectralon¹ sphere. Up to four lamps can be operated and the signals from two monitor photodiodes are recorded automatically.

3. Results

The measurements are described in Table 1. Two sets of SIRCUS studies were performed, in December 2000 and in December 2001. In November 2000, the LXR, SXR, and SXR-II measured the NPR on two separate days and were then calibrated on SIRCUS. For the December 2001 measurement set, the SXR-II and the VXR measured the NPR before and after the SIRCUS calibration, with multiple measurements of the individual radiance levels. FASCAL was used to calibrate the NPR in August 2000 and December 2001. The NPR four-lamp level saturates two of the channels in the SXR and the SXR-II, so measurements were not made for that configuration.

¹ Certain commercial equipment, instruments, or materials are identified in this paper to foster understanding. Such identification does not imply recommendation or endorsement by the National Institute of Standards and Technology, nor does it imply that the materials or equipment identified are necessarily the best available for the purpose.

The SIRCUS calibration results are sets of radiance responsivity values $R(\lambda)$ at the laser wavelengths used, with each set corresponding to one channel of one of the filter radiometers. For the in-band regions, the wavelength step was about 0.5 nm. Measurements from 380 nm or 400 nm to 930 nm with an interval of 5 nm to 10 nm determined the radiance response in the out-of-band region. The results were interpolated with a resolution of 0.2 nm using a cubic spline routine within the in-band region and linear interpolation for the out-of-band region. For the ETM+ channels in the LXR, linear interpolation was used for the in-band region.

The spectral radiance of the NPR, $L_{\text{NPR}}(\lambda)$, was measured over a broad spectral range, from 300 nm to 1000 nm or 1100 nm, every 25 nm. The values were interpolated onto the same wavelength grid as the $R(\lambda)$ values using a cubic spline routine. Then the predicted signal, S_p , was calculated using

$$S_p = \int R(\lambda) L_{\text{NPR}}(\lambda) d\lambda \quad (1)$$

and compared to the net measured signal, S_M . This process was repeated for every separate measurement of the different radiance levels for each of the 30 channels among the four filter radiometers (including the two separate SIRCUS calibrations of the SXR-II).

Determination of the uncertainty in the ratio S_p/S_M depends on the components described in Table 2. The components are associated with the $R(\lambda)$ values (SIRCUS, Ref. 4), the $L_{\text{NPR}}(\lambda)$ values (FASCAL, Ref. 8), numerical interpolation and integration, and the measurement repeatability. The robustness of the interpolation in $R(\lambda)$ over the in-band region was evaluated by comparing linear and cubic interpolation to the cubic spline. Interpolation in $L_{\text{NPR}}(\lambda)$ was tested using Planck's law to model the spectral

radiance. The measurement repeatability was evaluated from the multiple measurements of the same NPR illumination level in December 2000 or December 2001. The resulting standard deviations are between 0.03 % and 0.39 %, with the majority below 0.15 %. A few values are indicated in Fig. 1 using vertical lines. Given the small number of samples (two in most cases), the five VXR measurements of the brightest NPR level were used to estimate the measurement repeatability.

In addition to the identified uncertainty components, effects such as the radiance uniformity of the NPR or temporal changes in the radiance of the NPR (a factor in December 2000) are possible sources of bias. In addition, for the narrow band channels, the result of numerical evaluation of (1) is sensitive to the density and spacing of the SIRCUS values in the in-band region.

The results are shown in Fig. 1, with S_P/S_M plotted as a function of wavelength. For the wavelengths, we use the first moment of the interpolated responsivities. The average ratio for each NPR level is shown, and different symbols correspond to the filter radiometer, year measured, and NPR level. The ratios indicate that most results for S_P and S_M agree within the combined expanded uncertainties. There are outliers (SXR at 412 nm, +1.26 %, and LXR at 661 nm (narrowband), -1.12 %). The agreement for repeat SIRCUS measurements (SXR-II) or independently calibrated NPR radiance levels (LXR, SXR-II, and VXR) is good, typically 0.3 % to 0.5 %.

4. Summary

Four multichannel filter radiometers were used to compare the detector-based scale from SIRCUS to the source-based scale from FASCAL using the NPR as a transfer

source. The results agree within the combined expanded uncertainties, thus validating the accuracy of both the NIST detector-based and source-based methods. Work is in progress using filter radiometers with very narrow fields-of-view so that the blackbody standards can be addressed directly.

Acknowledgements. NASA's EOS Project Science Office (contract S-41365-F), SIMBIOS Project Office (contract S-64096-E) and the Landsat Project Office (contract S-44799-X) provided support for this work, in addition to the US Air Force Metrology (contracts 97-421 and 98-439).

References

1. Yoon, H. W., Gibson, C., Barnes, P. Y., *Appl. Optics*, 2002, **41**, 5879—5890.
2. Butler, J. J., Johnson, B. C., Brown, S. W., Yoon, H. W., Barnes, R. A., Markham, B. L., Biggar, S. F., Zalewski, E. F., Spyak, P. R., Cooper, J. W., and Sakuma, F., *Proc. SPIE*, 1999, **3870**, 180—192.
3. Johnson, B. C., Fowler, J. B., and Cromer, C. L., The SeaWiFS Transfer Radiometer (SXR), *NASA Tech. Memo. 1998—206892*, Vol. 1, (Edited by S. B. Hooker and E. R. Firestone), NASA/Goddard Space Flight Center, Greenbelt, Maryland, 1998, 58 pp.
4. Johnson, B. C., Brown, S. W., Eppeldauer, G. P., and Lykke, K. R., to appear in *Int. J. Remote Sensing*, 2002.
5. Markham, B. L., Schafer, J. S., Wood Jr., F. M., Dabney, P. W., and Barker, J. L., *Metrologia*, 1998, **35**, 643—648.
6. Meister, G., Abel, P., Barnes, R., Cooper, J., Davis, C., Godin, M., Goebel, D., Fargion, G., Frouin, R., Korwan, D., Maffione, R., McClain, C., McLean, S., Menzies, D., Poteau, A., Robertson, J., and Sherman, J., The First SIMBIOS Radiometric Intercomparison (SIMRIC-1), April—September 2001, *NASA/TM—2002-210006*, NASA/Goddard Space Flight Center, Greenbelt, Maryland, 60 pp.
7. Brown, S. W., Eppeldauer, G. P., and Lykke, K., R., *Metrologia*, 2000, **37**, 579—582.
8. Walker, J. H., Saunders, R., D., and Hattenburg, A., T., Spectral Radiance Calibrations. *NBS Special Publication 250-1*, U.S. Department of Commerce, National Institute of Standards and Technology, Washington, DC, 1987, 68 pp.

9. Brown, S. W., and Johnson, B., C., to appear in *Int. J. Remote Sensing*, 2002.

List of Tables

Table 1. The sequence of measurements in the comparison: the VXR measured the four lamp level five times and the two single lamp levels three times. The other filter radiometers were used twice with each level.

Table 2. Components of uncertainty associated with the ratio S_P/S_M . The values correspond to relative expanded uncertainty ($k = 2$) in percent.

List of Figures

Figure 1. The average values for the ratio S_P/S_M for each NPR level and SIRCUS measurement combination. The value in parenthesis in the legend indicates the NPR lamp configuration. For the SXR-II, the symbols correspond to: triangle—December 2000; diamond—December 2001.

Table 1. The sequence of measurements in the comparison: the VXR measured the four lamp level five times and the two single lamp levels three times. The other filter radiometers were used twice with each level.

Radiometer	SIRCUS Calibration	NPR Measurements	NPR Lamp Level	NPR Calibration
LXR	December 2000	November 2000	1—4 and 2	August 2000
SXR	December 2000	November 2000	2	August 2000
SXR-II	December 2000	November 2000	2	August 2000
SXR-II	December 2001	December 2001	2 and 3	December 2001
VXR	December 2001	December 2001	1—4, 2, and 3	December 2001

Table 2. Components of uncertainty associated with the ratio S_p/S_M . The values correspond to relative expanded uncertainty ($k = 2$) in percent.

Wavelength / nm	412	550	775	870
Component / %				
$R(I)$	0.25	0.25	0.25	0.25
$L_{NPR}(I)$	0.41	0.39	0.45	0.51
S_M	0.20	0.20	0.20	0.20
Interpolation	0.10	0.10	0.10	0.10
Expanded, $k = 2$	0.53	0.51	0.56	0.61

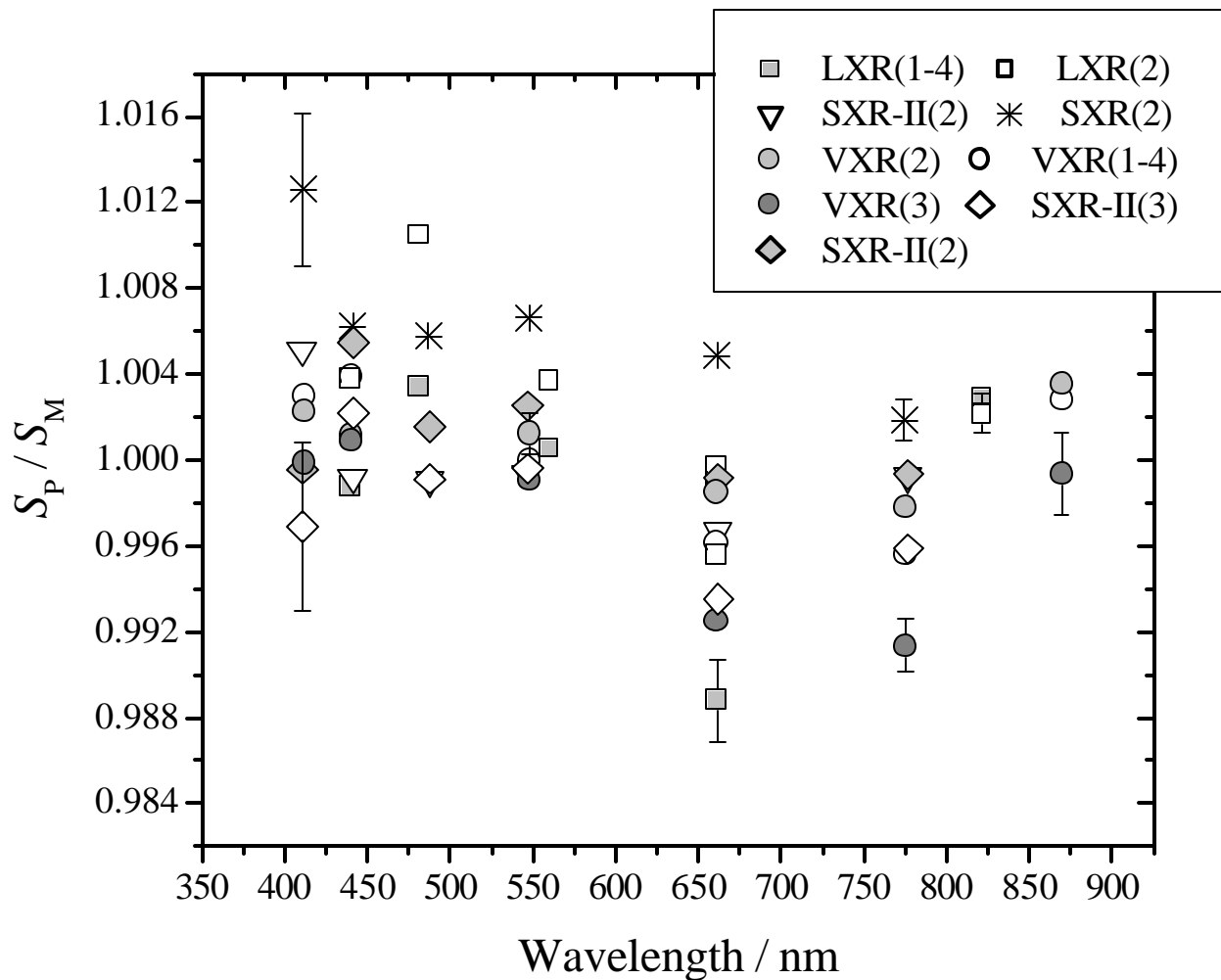


Figure 1. The average values for the ratio S_P/S_M for each NPR level and SIRCUS measurement combination. The value in parenthesis in the legend indicates the NPR lamp configuration. For the SXR-II, the symbols correspond to: triangle—December 2000; diamond—December 2001.